Int. J. Heat Mass Transfer. Vol. 23, pp. 1433–1445

0017–9310/80/1101–1433 $02.00/0

TAYLOR INSTABILITY IN BOILING, MELTING AND CONDENSATION OR EVAPORATION*

K. TAGHAVI-TAFRESHI and V. K. DHIR

Chemical, Nuclear and Thermal Engineering Department,
University of California, Los Angeles, CA 90024, U.S.A.

(*Received* 4 *December* 1979 *and in revised form* 5 *March* 1980)

Abstract — The combined effect of interfacial tension, liquid viscosity and liquid layer thickness on Taylor instability of plane horizontal interfaces has been studied. The linear analysis has been made keeping in mind the potential application of the results to physical processes such as boiling, melting of a horizontal substrate placed beneath pools of immiscible or miscible liquids and condensation or evaporation from horizontal plates or tubes. In all cases the predicted most dangerous wavelengths are compared with the available experimental data, and with limiting analytical results wherever possible. A few experiments have been conducted to substantiate the effect of liquid viscosity during dripping from horizontal tubes.

NOMENCLATURE

- B, function defined in equation (2);
- D, rod diameter;
- F, function defined in equation (28);
- g, gravitational constant;
- H, dimensionless layer height, $h[g(\rho_1 - \rho_2)/\sigma]^{1/2}$;
- $\bar{H}$, dimensionless layer height, $h(g/\nu^2)^{1/3}$;
- h, layer height;
- K, dimensionless wavenumber, $k[\sigma/g(\rho_1 - \rho_2)]^{1/2}$;
- $\bar{K}$, dimensionless wavenumber, $k(\nu^2/g)^{1/3}$;
- k, wavenumber;
- M, dimensionless viscosity parameter, $\sigma^{3/4}/[\nu g^{1/4}(\rho_1 - \rho_2)^{3/4}]$;
- m, dimensionless parameter defined in equation (16);
- p, pressure;
- R, density ratio, ρ_1/ρ_2;
- R', dimensionless rod radius, $D/2[\sigma/g(\rho_1 - \rho_2)]^{1/2}$;
- s, parameter equal to 1 for immiscible case and equal to 0 for miscible case;
- t, time;
- u, velocity in x-direction;
- v, velocity in y-direction;
- x, rectangular coordinate;
- y, rectangular coordinate.

Greek symbols

- η, interface irregularity;
- Λ, dimensionless wavelength, $1/\sqrt{3}K$;
- $\bar{\Lambda}$, dimensionless wavelength, $2\pi/\bar{K} = \lambda(g/\nu^2)^{1/3}$;
- λ, wavelength, $2\pi/k$;
- μ, viscosity;
- ν, kinematic viscosity;
- ρ, density;
- σ, interfacial tension;
- ϕ, stream function, defined in equations (7) and (8);
- ψ, potential function, defined in equations (7) and (8);
- Ω, dimensionless growth rate, $\omega\sigma^{1/4}(\rho_1 + \rho_2)^{1/2}/[g(\rho_1 - \rho_2)]^{3/4}$;
- Ω, dimensionless growth rate, $\omega(\nu/g)^{1/3}$;
- ω, growth rate.

Subscripts

- c, critical;
- d, most dangerous;
- t, derivative with respect to time;
- x, derivative with respect to x coordinate;
- y, derivative with respect to y coordinate;
- 1, upper layer;
- 2, lower layer.

Superscript

- T, transpose of a matrix.

INTRODUCTION

TAYLOR instability has been the subject of several studies in the past. These studies have generally sought simplifications to the complex interaction of such variables as finite fluid layer depth, fluid viscosity and interfacial tension. To properly analyze such phenomena as melting, condensation, evaporation, boiling and sublimation, it is, however, important that combined effect of these variables on the most dangerous wavelength and its growth rate be quantified. The purpose of this paper is to analyze the effect of viscosity, finite layer and surface tension on Taylor instability and to compare with data wherever possible.

* This work was supported by the Reactor Safety Research Division of the Nuclear Regulatory Commission under agreement No. AT(04-3)-34PA223, Mod. 5.

Instability of a horizontal interface between two inviscid and miscible fluids of infinite depth was discussed by Taylor [1] in 1950. He showed that irregularities at the interface tended to grow if acceleration was directed from heavier to less dense fluid. Later, Bellman and Pennington [2] extended the inviscid analysis to take into account the effect of surface tension and viscosity of the two fluids. For the simple case in which interfacial tension was included but fluids were assumed to be inviscid and infinite, they obtained the following dispersion relationship between dimensionless growth rate and dimensionless wave number as*

$$\Omega^2 = K - K^3 \tag{1}$$

Any disturbance with $K > 1$ will be stable while a disturbance with $K < 1$ will be unstable. For a neutral disturbance K will have value equal to 1 whereas for a disturbance having the fastest growth ($d\Omega/dK = 0$), K will correspond to $1/\sqrt{3}$.

From this formulation of the general case in which viscosity and surface tension were included, Bellman and Pennington [2] concluded that effect of viscosity was to elongate the fastest growing wavelength. Viscosity did not, however, effect the wavelength of a neutral wave. Subsequently Dhir and Lienhard [3] used Bellman and Pennington's analysis to obtain a dispersion relation as

$$B(M_1, M_2) \equiv (-K + K^3 + \Omega^2) \times \left(\frac{1}{\dfrac{1}{M_1} + \dfrac{m_1}{RM_2}} + \frac{1}{\dfrac{1}{RM_2} + \dfrac{m_1}{M_1}} \right) + \frac{4\Omega K^2 R}{(R^2-1)^{1/2}} = 0. \tag{2}$$

Assuming that fluid layers were infinite and that vapor viscosity could be neglected, Dhir and Lienhard [3] showed that their data of dominant wavelength observed during film boiling of cyclohexanol compared quite favorably with the data.

The effect of heat and mass transfer on instability of two finite layers of inviscid liquids was analyzed by Hsieh [4]. His work showed that for many applications of interest, the effect of heat and mass transfer on the fastest growing Taylor wavelength and its growth rate, will be small. For the limiting case of no heat and mass transfer at the interface, his expression for the dispersion relation approached the earlier result of Lamb [5]

$$\Omega^2 = \frac{(R+1)(K-K^3)}{R \coth KH_1 + \coth KH_2}. \tag{3}$$

From equation (3), it is seen that finite layer height has no effect on the critical wave number ($\Omega = 0$) but tends to decrease growth rate while increasing the wave number of the fastest growing Taylor wave. In the limit as H_2 goes to zero, the dimensionless wave number of the fastest growing wave approaches $1/\sqrt{2}$.

* Symbols are defined in the Nomenclature.

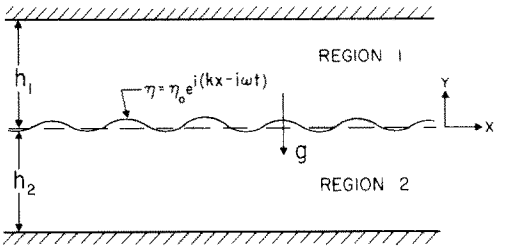

FIG. 1. Model for stability analysis.

Plesset and Whipple [6] made the first attempt to study the combined effect of fluid viscosity and layer height on Taylor instability. Since the motivation of their work was to explain certain bio-convective phenomena, they were interested in stability of superposed layers of miscible liquids of near equal viscosities and densities. Their analysis showed, however, that viscosity tended to elongate the fastest growing wavelength while finite layer height tended to shorten the wavelength.

In this paper first dispersion relations for the most general case in which both superposed layers are assumed to be finite, viscous and immiscible is obtained. The dispersion relation which is a determinant of an 8 × 8 matrix is then simplified to treat physical phenomena of practical interest such as boiling, sublimation, condensation and melting. The predictions are then compared with experimental data wherever possible. Finally, it is shown how instability of miscible fluids could easily be analyzed using the dispersion relation obtained earlier for immiscible fluids.

ANALYSIS

Two-dimensional instability analysis of two superposed layers is made by using the physical model shown in Fig. 1. For most of the applications, this assumption is justified because the cell size given by a two-dimensional wave will be the same as that given by a three-dimensional wave. This has been shown by Sernas *et al.* [7] for film boiling on a flat plate. The fluids are bounded by rigid wall and are assumed to be incompressible and Newtonian. Non-linearity effects are neglected. This assumption is not very stringent in the absence of heat and mass transfer at the interface. It is expected that once a wave pattern is established, the non-linearity in growth rate will not alter the dominant wavelength. The linearized governing equations for both fluids are:

$$u_x + v_y = 0 \tag{4}$$

$$u_t + \frac{1}{\rho} p_x = \nu(u_{xx} + u_{yy}) \tag{5}$$

$$v_t + \frac{1}{\rho} p_y + g = \nu(v_{xx} + v_{yy}). \tag{6}$$

These equations are satisfied by

$$u = -\phi_x - \psi_y \tag{7}$$

$$v = -\phi_y + \psi_x \tag{8}$$

$$p = p_0 - \rho g y + \rho \phi_t \tag{9}$$

provided that

$$\phi_{xx} + \phi_{yy} = 0 \tag{10}$$

$$\frac{\mu}{\rho}(\psi_{xx} + \psi_{yy}) = \psi_t. \tag{11}$$

In the above equations ϕ and ψ are potential and stream functions while p_0 is pressure at the undisturbed interface. Equations (10) and (11) can be satisfied if ϕ and ψ for the upper and lower fluid are chosen as

$$\phi_1 = [A_1 e^{k(y-h_1)} + B_1 e^{-k(y-h_1)}]e^{\omega t} \cos kx \tag{12}$$

$$\psi_1 = [C_1 e^{m_1 k(y-h_1)} + D_1 e^{-m_1 k(y-h_1)}]e^{\omega t} \sin kx \tag{13}$$

$$\phi_2 = [A_2 e^{k(y+h_2)} + B_2 e^{-k(y+h_2)}]e^{\omega t} \cos kx \tag{14}$$

$$\psi_2 = [C_2 e^{m_2 k(y+h_2)} + D_2 e^{-m_2 k(y+h_2)}]e^{\omega t} \sin kx \tag{15}$$

and parameters m_1 and m_2 involving growth rate and wave numbers are defined as

$$m_i = \left(k^2 + \frac{\omega}{\nu_i k^2}\right)^{1/2} \quad i = 1,2. \tag{16}$$

The linearized kinematic condition at the interface can be written as:

$$\eta_t = v \quad \text{at } y = \eta \tag{17}$$

while the boundary conditions at the perturbed interface and at the boundary walls are:

$$u_1 = u_2 \quad \text{at } y = \eta \left.\right\} \text{no slip condition} \tag{18}$$

$$v_1 = v_2 \quad \text{at } y = \eta \left.\right\} \text{at interface} \tag{19}$$

$$-p_1 + 2\mu_1 v_{1,y} = -p_2 + 2\mu_2 v_{2,y} - \sigma \eta_{xx}$$

$$\mu_1(v_{1,x} + u_{1,y}) = \mu_2(v_{2,x} + u_{2,y})$$

$$\text{at } y = \eta \left.\right\} \text{equal stress components} \tag{20}$$

$$\text{at } y = \eta \left.\right\} \text{at interface} \tag{21}$$

$$u_2 = 0 \quad \text{at } y = -h_2 \left.\right\} \text{no slip condition} \tag{22}$$

$$v_2 = 0 \quad \text{at } y = -h_2 \left.\right\} \text{at lower boundary} \tag{23}$$

$$u_1 = 0 \quad \text{at } y = h_1 \left.\right\} \text{no slip condition} \tag{24}$$

$$v_1 = 0 \quad \text{at } y = h_1 \left.\right\} \text{at upper boundary.} \tag{25}$$

Substitution of kinematic condition (17) and potential and stream functions given by equations (12)–(15) into the above interfacial and bounding wall conditions yields eight equations in eight unknowns. These equations can be written in the form

$$[C][A_1, B_1, C_1, D_1, A_2, B_2, C_2, D_2]^T = 0. \tag{26}$$

For a non-trivial solution the determinant of the coefficient matrix, C, should be equal to zero. After non-dimensionalizing various parameters and rearranging various elements of the matrix, C, the dispersion relation between growth rate, Ω, and wavenumber, K, is obtained as shown in equation (27)

$$\det[C] \equiv \begin{vmatrix} 1 & 1 & -m_1 & m_1 & -1 & -1 & m_2 & -m_2 \\ -1 & 1 & 1 & 1 & 1 & -1 & -1 & -1 \\ -F-\Omega^2\frac{m_1^2+1}{m_1^2-1} & F-\Omega^2\frac{m_1^2+1}{m_1^2-1} & F+\Omega^2\frac{2m_1}{m_1^2-1} & F-\Omega^2\frac{2m_1}{m_1^2-1} & \frac{\Omega^2}{R}\frac{m_2^2+1}{m_1^2-1} & \frac{\Omega^2}{R}\frac{m_2^2+1}{m_2^2-1} & \frac{-\Omega^2}{R}\frac{2m_2}{m_2^2-1} & \frac{\Omega^2}{R}\frac{2m_2}{m_2^2-1} \\ 2 & -2 & -(m_1^2+1) & -(m_1^2+1) & \frac{-2}{R}\frac{M_1}{M_2} & \frac{2}{R}\frac{M_1}{M_2} & \frac{m_2^2+1}{R}\frac{M_1}{M_2} & \frac{m_2^2+1}{R}\frac{M_1}{M_2} \\ 0 & 0 & 0 & 0 & e^{-KH_2} & e^{KH_2} & -m_2 e^{-m_2 KH_2} & m_2 e^{m_2 KH_2} \\ 0 & 0 & 0 & 0 & -e^{-KH_2} & e^{KH_2} & e^{-m_2 KH_2} & e^{m_2 KH_2} \\ e^{KH_1} & e^{-KH_1} & -m_1 e^{m_1 KH_1} & m_1 e^{-m_1 KH_1} & 0 & 0 & 0 & 0 \\ e^{KH_1} & -e^{-KH_1} & -e^{m_1 KH_1} & -e^{-m_1 KH_1} & 0 & 0 & 0 & 0 \end{vmatrix} = 0 \tag{27}$$

where

$$m_i = 1 + \frac{\Omega M_i}{K^2}[(R-1)/(R+1)]^{1/2} \quad i = 1,2 \tag{16a}$$

and

$$F(K) = \frac{R+1}{R}(K - sK^3). \tag{28}$$

In equation (28) s is set equal to 1 in presence of interfacial tension and is set equal to 0 when the two fluids are miscible.

The dispersion relation, equation (27), has the following properties:

(i) it reduces to equation (1) if $M_1 = M_2 = H_1 = H_2 = \infty$.

(ii) it reduces to equation (2) if $H_1 = H_2 = \infty$.

(iii) it reduces to equation (3) if $M_1 = M_2 = \infty$.

Equation (27) represents the most general situation and could be solved numerically to determine the role of such variables as M_1, M_2, H_1, H_2, and R in the fastest growing wavelength and on the corresponding growth rate. Fortunately, only rarely has one to do so since most of the phenomena of interest lend themselves to some sort of simplifications to equation (27). For example, during film boiling on a flat plate or a cylinder, the vapor could be assumed inviscid while the overlying liquid layer height could be assumed as

infinite. Similarly, during condensation or evaporation from a tube or flat plate, the vapor layer could be considered inviscid and infinite. Next, we discuss several simplified cases of equation (27) while keeping in mind their potential application to physical phenomena of interest.

1. *Infinite layer viscous, finite layer inviscid*

Using the simplification that $H_1 \to \infty$ and $M_2 \to \infty$, the dispersion relation (27) reduces to

$$\begin{vmatrix} 1 & \frac{1}{\Omega^2}\frac{m_2+1}{m_2-1} & \frac{-1}{\Omega^2}\frac{m_2+1}{m_2-1} & \frac{-1}{\Omega^2}\frac{2m_2}{m_2-1} & \frac{-1}{\Omega^2}\frac{2m_2}{m_2-1} \\ F-\Omega^2 & \frac{1}{R}\frac{m_2+1}{m_2-1} & \frac{1}{R}\frac{m_2+1}{m_2-1} & -\frac{1}{R}\frac{2m_2}{m_2-1} & \frac{1}{R}\frac{2m_2}{m_2-1} \\ 0 & -2 & 2 & m_2+1 & m_2+1 \\ 0 & e^{-KH_2} & e^{KH_2} & -m_2 e^{-m_2KH_2} & m_2 e^{m_2KH_2} \\ 0 & -e^{-KH_2} & e^{KH_2} & e^{-m_2KH_2} & e^{m_2KH_2} \end{vmatrix} = 0. \tag{32}$$

The determinant equation (32) could be expanded. After several complicated algebraic manipulations equation (32) reduces to:

$$B(\infty, M_2) - \frac{\Omega K^2 R}{(R^2-1)^{1/2}} \frac{m_2+1}{m_2} \times \left\{ \frac{4m}{m_2+1} + m_2^2 - 1 + \frac{-8m(m_2^2+1) + [(m_2^2+1)^2 - 4m_2](m_2-1)\cosh(m_2+1)KH_2 + [(m_2^2+1)^2 + 4m_2](m_2+1)\cosh(m_2-1)KH_2}{(m_2^2-1)[(m_2+1)\sinh(m_2-1)KH_2 - (m_2-1)\sinh(m_2+1)KH_2]} \right\} = 0 \tag{33}$$

$$\begin{vmatrix} 1 & 1 & 1 & -1 \\ F-\Omega^2\frac{m_1^2+1}{m_1^2-1} & F-\Omega^2\frac{2m_1}{m_1^2-1} & \frac{\Omega^2}{R} & \frac{\Omega^2}{R} \\ -2 & -(m_1^2+1) & 0 & 0 \\ 0 & 0 & -e^{-2KH_2} & 1 \end{vmatrix} = 0. \tag{29}$$

The determinant in equation (29) could be expanded into

$$B(M_1, \infty) + (\coth KH_2 - 1)\Omega^2 \frac{M_1}{R+1} \frac{m_1+1}{m_1} = 0 \tag{30a}$$

or

$$-K + K^3 + \Omega^2 \times \left\{ 1 + \frac{4R}{R+1} \frac{1}{m_1^2-1} \frac{m_1}{m_1+1} + \frac{\coth KH_2 - 1}{R+1} \right\} = 0. \tag{30b}$$

The first term in equation (30a) is Bellman and Pennington's equation (2) with $M_2 = \infty$. The second term represents the correction due to lower layer being finite. In the limit as H_2 goes to infinity the second term vanishes. To find the most dangerous growth rate and corresponding wavenumber, equation (30b) could be differentiated with respect to K while setting $d\Omega/dK = 0$ in it. This new equation along with equation (30b) could be solved simultaneously for Ω_d and K_d. A closed form analytical solution could not be obtained for Ω_d and K_d, hence the two equations in two unknowns Ω and K have to be solved numerically. However, analytical solution for the limiting case as $H_2 \to 0$ are obtained as

$$K_d = 1/\sqrt{2} \text{ (irrespective of value of } M_1) \quad \text{as } H_2 \to 0. \tag{31}$$
$$\Omega_d \to [(R+1)H_2/2]^{1/2}$$

These results have been verified with numerical solution and will be discussed in the section on results and discussion.

2. *Finite layer viscous, infinite layer inviscid*

Assuming that H_1 and $M_1 \to \infty$, the dispersion relation (27) reduces to

$$\begin{vmatrix} 1 & \frac{1}{\Omega^2}\frac{m_2+1}{m_2-1} & \frac{-1}{\Omega^2}\frac{m_2+1}{m_2-1} & \frac{-1}{\Omega^2}\frac{2m_2}{m_2-1} & \frac{-1}{\Omega^2}\frac{2m_2}{m_2-1} \\ F-\Omega^2 & \frac{1}{R}\frac{m_2+1}{m_2-1} & \frac{1}{R}\frac{m_2+1}{m_2-1} & -\frac{1}{R}\frac{2m_2}{m_2-1} & \frac{1}{R}\frac{2m_2}{m_2-1} \\ 0 & -2 & 2 & m_2+1 & m_2+1 \\ 0 & e^{-KH_2} & e^{KH_2} & -m_2 e^{-m_2KH_2} & m_2 e^{m_2KH_2} \\ 0 & -e^{-KH_2} & e^{KH_2} & e^{-m_2KH_2} & e^{m_2KH_2} \end{vmatrix} = 0. \tag{32}$$

The determinant equation (32) could be expanded. After several complicated algebraic manipulations equation (32) reduces to:

$$B(\infty, M_2) - \frac{\Omega K^2 R}{(R^2-1)^{1/2}} \frac{m_2+1}{m_2} \times \left\{ \frac{4m}{m_2+1} + m_2^2 - 1 + \frac{-8m(m_2^2+1) + [(m_2^2+1)^2 - 4m_2](m_2-1)\cosh(m_2+1)KH_2 + [(m_2^2+1)^2 + 4m_2](m_2+1)\cosh(m_2-1)KH_2}{(m_2^2-1)[(m_2+1)\sinh(m_2-1)KH_2 - (m_2-1)\sinh(m_2+1)KH_2]} \right\} = 0 \tag{33}$$

The first term of equation (33) is again Bellman and Pennington's equation (2) with $M_1 = \infty$. The second term in equation (33) represents the correction to the dispersion relation due to one of the layers being finite. Equation (33) has to be solved numerically for the most dangerous wavelength and the corresponding growth rate, as analytical solutions are not possible. However, in the limit as $H_2 \to 0$, the analytical solutions for the wavenumber and growth rate of the most susceptible wave are obtained as

$$K_d \to 1/\sqrt{2}$$
$$\Omega_d \to \frac{M_2(R^2-1)^{1/2}H_2^3}{12} \tag{34}$$

provided that

$$M_2(R-1)H_2^3 \ll 1.$$

It may be pointed out that dispersion relation (33) was obtained when the lower lighter layer was viscous and finite. This equation will still be valid if the finite viscous layer was heavier and the orientation of the two fluids was reversed. However, R in equation (33) would have to be replaced by $1/R$.

3. *Finite layer, viscous, infinite layer viscous*

Assuming that upper layer is infinite such that $H_1 \to \infty$, the dispersion relation (27) reduces to

$$\begin{vmatrix} 1 & m_1 & -1 & -1 & m_2 & m_2 \\ 1 & 1 & 1 & -1 & -1 & -1 \\ F-\Omega^2\dfrac{m_1^2+1}{m_1^2-1} & F-\Omega^2\dfrac{2m_1}{m_1^2-1} & \dfrac{\Omega^2}{R}\dfrac{m_2^2+1}{m_2^2-1} & \dfrac{\Omega^2}{R}\dfrac{m_2^2+1}{m_2^2-1} & -\dfrac{\Omega^2}{R}\dfrac{2m_2}{m_2^2-1} & \dfrac{\Omega^2}{R}\dfrac{2m_2}{m_2^2-1} \\ -2 & -(m_1^2+1) & \dfrac{-2}{R}\dfrac{M_1}{M_2} & \dfrac{2}{R}\dfrac{M_1}{M_2} & \dfrac{m_2^2+1}{R}\dfrac{M_1}{M_2} & \dfrac{m_2^2+1}{R}\dfrac{M_1}{M_2} \\ 0 & 0 & e^{-KH_2} & e^{KH_2} & -me^{-m_2KH_2} & m_2e^{m_2KH_2} \\ 0 & 0 & -e^{-KH_2} & e^{KH_2} & e^{-m_2KH_2} & e^{m_2KH_2} \end{vmatrix} = 0. \quad (35)$$

The most dangerous wavelength and its growth rate could only be obtained by solving the dispersion relation numerically. In the present work this was done for the case when kinematic viscosities of the two fluids are assumed to be the same.

4. *Miscible fluids with finite layer viscous, infinite layer viscous*

In many applications the superposed layers as envisioned in case 3 may be such that the two fluids are miscible. For this case the dispersion relation (35) could still be used by simply letting $s = 0$ in function F. Now the surface tension, σ, has no physical meaning and it may be taken as a constant which simply cancels out*. The resulting dimensionless growth rate, wavenumber and layer height based on kinematic viscosity of one of the layers are,

$$\bar{\Omega} = \omega(\nu_i/g^2)^{1/3} \quad (36)$$

$$\bar{K} = k(\nu_i^2/g)^{1/3} \quad i = 1 \text{ or } 2 \quad (37)$$

and

$$\bar{H} = h(g/\nu_i^2)^{1/3}. \quad (38)$$

While the parameters m_1 and m_2 reduce to

$$m_j = \left(1 + \frac{\bar{\Omega}}{\bar{K}^2}\frac{\nu_j}{\nu_i}\right)^{1/2} \quad \begin{matrix} i = 1 \text{ or } 2 \\ j = 1 \text{ and } 2. \end{matrix} \quad (39)$$

numerically for wavenumber and growth frequency of the disturbance most susceptible to growth by using subroutine ZSYSTM. This subroutine solves simultaneously n-non-linear equations in n unknowns. The calculations are repeated for various fluid viscosity parameters, M_1 and M_2, density ratios, R, and fluid layer heights, H_1 and H_2. The variations in the numerical values of the parameters are strongly guided by the potential application of the results to various physical processes. The results are plotted in terms of the dimensionless most dangerous wavelength ($\Lambda_d = 1/\sqrt{3}\ K_d$), rather than wavenumber because wavelengths are measured directly in the experiments. Dominant disturbances generally become nonlinear after a short initial period of linear growth. The present linear analysis is not apt to describe long time growth rate or the average growth rate. Hence growth rates have generally not been plotted as for any application average growth rate must be determined from experiments. The nonlinearity or growth rate is, however, not expected to alter the dominant wavelength.

Boiling

During film boiling on a flat plate or during pseudo film boiling on a slab of dry ice [8], vapor or gas layer

The dispersion relation (35) with this non-dimensionalizing scheme becomes

$$\begin{vmatrix} 1 & m_1 & -1 & -1 & m_2 & m_2 \\ 1 & 1 & 1 & -1 & -1 & -1 \\ \bar{K}\dfrac{R-1}{R}-\bar{\Omega}^2\dfrac{m_1^2+1}{m_1^2-1} & \bar{K}\dfrac{R-1}{R}-\bar{\Omega}^2\dfrac{2m_1}{m_1^2-1} & \dfrac{\bar{\Omega}^2}{R}\dfrac{m_2^2+1}{m_2^2-1} & \dfrac{\bar{\Omega}^2}{R}\dfrac{m_2^2+1}{m_2^2-1} & -\dfrac{\bar{\Omega}^2}{R}\dfrac{2m_2}{m_2^2-1} & \dfrac{\bar{\Omega}^2}{R}\dfrac{2m_2}{m_2^2-1} \\ -2 & -(m_1^2+1) & -\dfrac{2}{R}\dfrac{\nu_2}{\nu_1} & \dfrac{2}{R}\dfrac{\nu_2}{\nu_1} & \dfrac{m_2^2+1}{R} & \dfrac{m_2^2+1}{R}\dfrac{\nu_2}{\nu_1} \\ 0 & 0 & e^{-\bar{K}\bar{H}_2} & e^{\bar{K}\bar{H}_2} & -m_2e^{-m_2\bar{K}\bar{H}_2} & m_2e^{m_2\bar{K}\bar{H}_2} \\ 0 & 0 & -e^{-\bar{K}\bar{H}_2} & e^{\bar{K}\bar{H}_2} & e^{-m_2\bar{K}\bar{H}_2} & e^{m_2\bar{K}\bar{H}_2} \end{vmatrix} = 0. \quad (40)$$

RESULTS AND DISCUSSION

The dispersion relations developed in the previous section along with their derivatives with respect to wavenumber (with $d\Omega/dK$ set equal to 0) were solved

separates the solid surface from an overlying liquid pool. The thickness of the vapor or gas layer is generally small whereas the depth of the pool or overlying liquid is relatively quite large. The viscosity of vapor is negligible in comparison to that of the liquid. Thus, film boiling can be represented by case 1 in which a lower layer is assumed to be inviscid and

* Details are shown in Appendix A.

finite while the upper layer is assumed to be viscous and infinite. The dimensionless most dangerous wavelength obtained by solving dispersion relation equation (30b) is plotted in Fig. 2 as a function of vapor or gas blanket thickness. The calculations are made to represent film boiling at low pressure ($R > 200$) and at pressures near critical ($R \simeq 1.1$). It is clear from Fig. 2 that irrespective of the value of the liquid vapor density ratio and the liquid viscosity parameter, M_1, the most dangerous wavelength goes to $\sqrt{2/3}$ as vapor blanket thickness goes to zero. This value is the same as predicted earlier in the analysis section. For large density ratios the effect of vapor blanket thickness on wavelength is much less pronounced. The dimensionless vapor blanket thickness of about 0.05 ($\simeq$0.1 mm for water vapor at 1 atm pressure) acts as infinite for $R \geq 200$ and for values of M_1 up to 0.1. Vapor blanket thicknesses observed during film boiling are generally larger than this value and it proves that the assumption of infinite vapor blanket thickness made earlier by Dhir and Lienhard [3] during film boiling of viscous liquids was correct. For density ratios of the order of about 1, vapor blanket thickness acting as infinite depends strongly on the viscosity of the overlying liquid. Interacting effect of liquid viscosity and density ratio on wavelength is obtained by noting that for $M_1 < 100$, the asymptotic value of the most dangerous wavelength depends on the liquid–vapor density ratio. It may be pointed out that liquids with $M_1 > 100$ behave as inviscid and wavelengths plotted in Fig. 2 for $M_1 \geq 100$ are the same as would be obtained from Hsieh's [4] inviscid analysis without heat and mass transfer at the interface.

In Fig. 2, two data points obtained during sublimation of a horizontal slab of dry ice [8] placed beneath a pool of water or glycerol are also plotted. The ratio of liquid to gas densities in these cases were 580 and 730 whereas liquid viscosity parameter M_1, for water was 440 for glycerol it was 10. The gas blanket thickness in each case was calculated from known values of the average heat transfer coefficient and by assuming that the gas film had no inertia. It is noted that observed values of wavelength compare favorably with the data. Unfortunately, the values of viscosity parameter, M_1, and dimensionless gas film thickness H_1 are such that no appreciable effect of liquid viscosity and finite layer height can be found. For these data inviscid-infinite fluid layer analysis would have yielded equally good predictions.

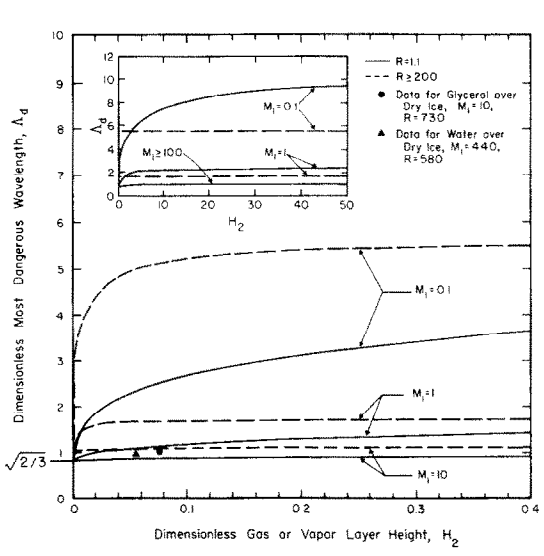

FIG. 2. Effect of finite vapor layer height on the most dangerous Taylor wavelength observed during film boiling.

Melting of horizontal substrate placed beneath a pool of heavier immiscible liquid

During different stages of progression of a hypothetical core disruptive accident in nuclear reactors, molten fuel or fuel steel mixture may come in contact with horizontal structural material (steel) or with sacrificial material in a core catcher or with concrete floor of the containment. Heat transfer from the overlying liquid pool will cause melting of the supporting substrate. If a solid crust does not separate the pool from the melting substrate, the melt which is generally lighter than the pool will be removed by Taylor instability. The melt removal configuration in turn will govern the penetration rate of the pool into the solid. The hydrodynamic and thermal processes associated with melting of lighter materials placed beneath a pool of heavier immiscible liquid were investigated in [9]. In this study a pool of water was formed over a slab of frozen olive oil ($\rho_{water}/\rho_{olive\ oil} \simeq 1.1$). Figure 3 taken from [9] clearly shows a Taylor wave pattern during melting of a slab of olive oil.

In a melting process such as described above and shown in Fig. 3, a thin melt layer separates the solid from the overlying liquid. The melt is generally viscous whereas the overlying liquid in most cases can be assumed to be inviscid. Also, the liquid pool is much deeper than the melt layer. Such a situation is represented by case 2 in which a finite layer of viscous and lighter liquid lies beneath an infinite layer of heavier inviscid liquid. Figure 4 shows the most dangerous wavelength as a function of melt layer thickness for different melt viscosity parameters, M_2, and for pool to melt density ratio, R, of 1.1 (water over olive oil) and 4. It is noted that the effect of reduced melt layer thickness is to shorten the most dangerous wavelength. Again, as predicted from the analysis, the most dangerous wavelength irrespective of magnitude of the melt layer viscosity and pool to melt density ratio goes to $\sqrt{2/3}$ as the melt layer, H_2, approaches zero. For thicker melt layers ($H_2 \to \infty$), the effect of liquid viscosity is to damp the growth rate of the disturbance which in turn results in longer most dangerous wavelengths. The effect of melt viscosity on the most dangerous wavelength diminishes, however, as the pool to melt density ratio becomes large. The results of numerical calculations for $R \to \infty$ (although not plotted in Fig. 4) show that the most dangerous wavelength will approach the inviscid case irrespective

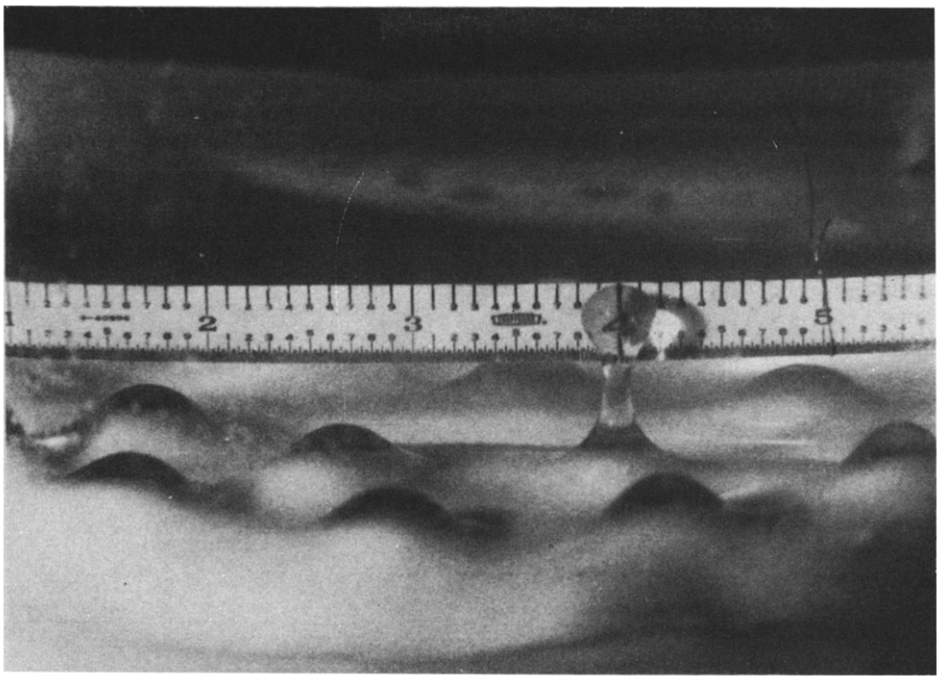

FIG. 3. Photograph of melting of a horizontal slab of frozen olive oil placed beneath a pool of warm water.

of the viscosity of the melt as long as the melt layer is not too thin. These calculations confirm that the earlier assumption that vapor is inviscid during film boiling will have only second order effect on the most dangerous wavelength and suggest that RM_2 may be the most relevant parameter for determining the effect of viscosity of the lower layer. The interacting effects of melt viscosity and melt layer thickness on the most dangerous wavelength is more clearly demonstrated if, for $R = 4$, the dependence of wavelength or melt layer height is compared between liquid viscosity parameters $M_2 = 10$ and 100. For melt layer thickness less than 1.2, the predicted wavelengths for $M_2 = 10$ are shorter than for $M_2 \geq 100$. The reason for this peculiar behavior is that as the melt layer becomes thin, the viscous drag in the film becomes important. With the constraints imposed by surface tension and buoyancy, shorter wavelengths offering less viscous drag are preferred.

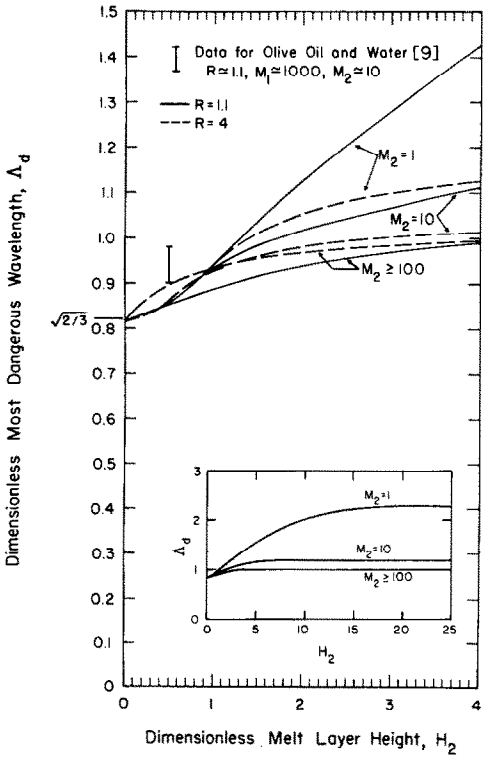

FIG. 4. Prediction of Taylor wavelength during melting of horizontal substrate placed beneath a pool of heavier immiscible inviscid liquid.

In Fig. 4, the range of wavelengths [9] observed during melting of a slab of olive oil ($M_2 = 10$) placed beneath a pool of water ($M_1 = 1100$), is also plotted. It is found that observed wavelengths are about 5–15% longer than predicted. This agreement is indeed good noting that the difference is within uncertainty of the data. The observed wavelengths would have been about 25% shorter, had the melt layer been assumed to be infinite. The effect of finite layer is much more pronounced if one compares the growth rates given by both finite and infinite layer analysis. The growth rate as a function of melt layer thickness for olive oil water combination is shown in Fig. 5. For a melt layer thickness $H_2 = 0.5$ ($H_2^3 = 0.125$), the finite layer analysis gives dimensionless growth rate of 0.04 whereas infinite layer analysis would have predicted it to be 0.86. The experimentally observed interface growth rate [9] during the period of linear growth compares quite favorably with the finite melt layer prediction. The analytically predicted growth rate as $H_2 \rightarrow 0$ is

also fully substantiated by the numerical solutions.

In situations where the viscosity of the overlying liquid pool cannot be neglected, dispersion relation equation (35) would be applicable. Figure 6 shows the most dangerous wavelength as a function of melt layer height when both melt and overlying liquids are viscous or when viscosity of either melt or overlying liquid pool can be ignored. The calculations are made for pool to melt density ratios of 1.1 and 4. In all cases the dimensionless wavelength goes to $\sqrt{2/3}$ as the thickness of the melt layer approaches zero. However, the limiting behavior of wavelengths depends strongly on the relative viscosities and density ratio of the two liquids. For melt layer heights less than 2, the viscosity of the overlying liquid has little effect on the most dangerous wavelength because as the layer becomes thin viscous dissipation in the melt layer determines the wavelength. As the melt layer height becomes large, viscosities of both liquids affect the most dangerous wavelength. In the asymptotic limit, the wavelength for an inviscid pool is about 15% shorter than for a pool with viscosity parameter $M_1 = 10$. It is interesting to note that for nearly equal pool to melt densities (e.g. $R = 1.1$) the asymptotic wavelength is the same when either one of the two liquids is assumed to be inviscid. The effect of increased pool to melt density ratio is to diminish the effect of viscosity of either of the two liquids on the most dangerous wavelength.

Condensation or evaporation from the underside of a horizontal flat plate or large diameter horizontal tubes

Heat transfer during condensation on a downward facing plate [10] or the break up of droplets from the underside of a bank of tubes in an evaporator [11] will be governed by Taylor instability. The condensate or the evaporating liquid is much more viscous than the surrounding vapor. The vapor layer is generally very deep whereas the liquid film is thin. For tubes with $R' > 2$, the effect of the radius of curvature of the tube on dominant wavelength is expected to be very small [12]. Liquid vapor interface on tubes with $R' > 2$ can be assumed to be plane without any loss of accuracy.

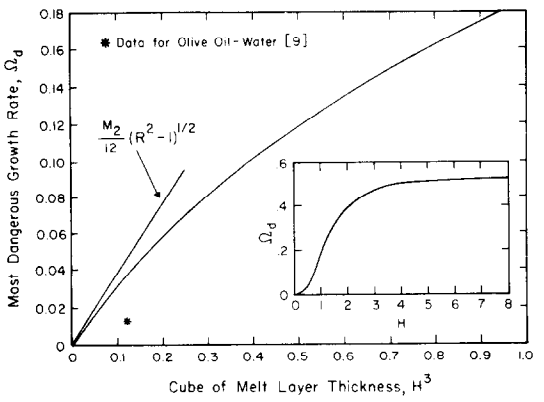

FIG. 5. Dependence of Taylor wave growth rate on melt layer height when the overlying liquid is assumed to be immiscible and inviscid ($M_2 = 10$, $R = 1.1$).

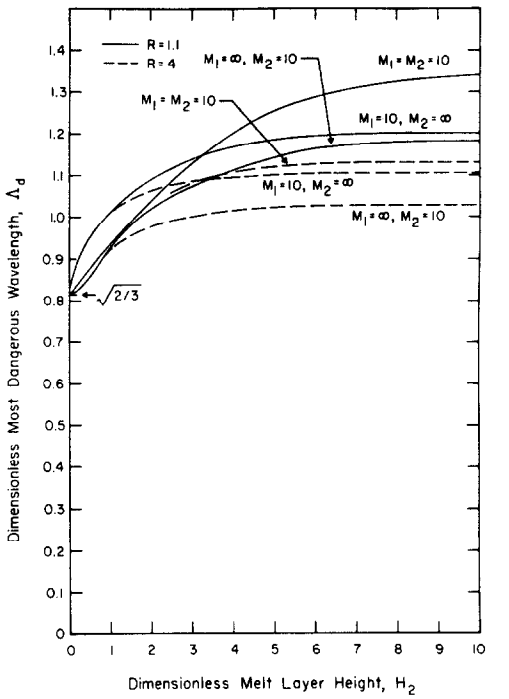

FIG. 6. Effect of melt and overlying liquid pool viscosity on the most dangerous Taylor wavelength.

Thus condensation or evaporation is similar to melting of immiscible liquids discussed earlier, except now the density ratio, R, is much less than unity and direction of gravity is reversed. Thus, the dispersion relation equation (33) can again be used to determine the most dangerous wavelength as a function of liquid

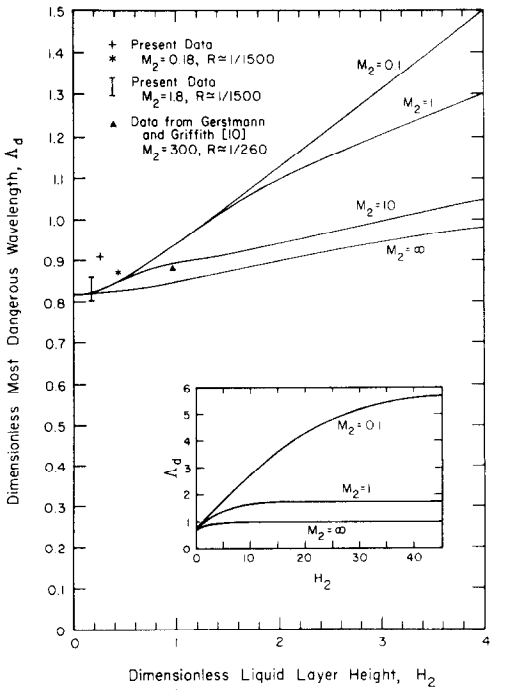

FIG. 7. Dependence of the most dangerous Taylor wavelength on condensate layer height and viscosity.

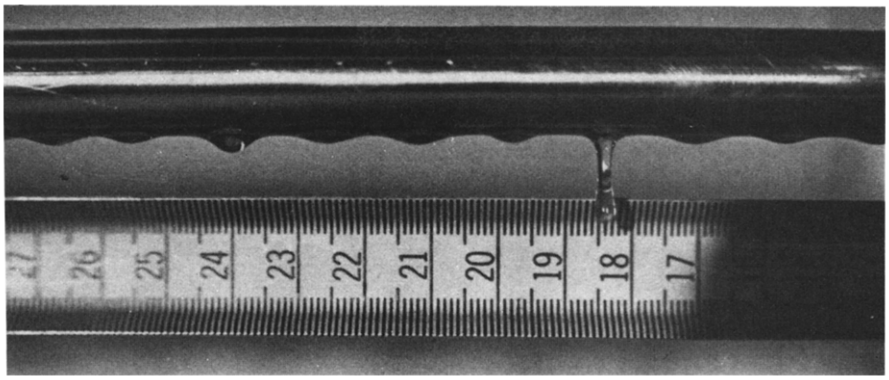

FIG. 8. Photograph of Taylor wave pattern observed during dripping off of silicone oil from a 1.25 cm dia rod

film thickness for different liquid viscosity parameters, M_2. The results of these calculations are plotted in Fig. 7 for $R \leq 1/200$. The effect of liquid viscosity is to increase the wavelength whereas finite melt layer tends to shorten the wavelength. The limiting value of the wavelength as film layer thickness goes to zero is again governed by surface tension and buoyancy. The interacting effect of buoyancy, surface tension and viscosity results in a point of inflection in the curves. The liquid layer depth at which this point of inflection occurs depends on liquid viscosity as is the depth at which the liquid layer acts as infinite.

A few dripping experiments with highly viscous silicone oils were conducted on 1.25 cm ($R' = 3.5$) dia rod. In the experiments the flow rate of the liquid dripping from the rod could be controlled. The details of the experiments are given in Appendix B. The wavelengths measured at low flow rates* are plotted in Fig. 7 while a typical wavepattern observed on the rod is shown in Fig. 8. It is noted that the data obtained with $M_2 = 1.8$ and 0.18 lie within -2% and $+1\%$ of the predictions. However, the predictions based on infinite liquid layer depth would have been in error by about 100% for $M_2 = 1.8$ and by 500% for $M = 0.18$. Ironically, the liquid film thickness around the rods in both cases is such that predictions based on infinite-inviscid layer analysis would have been in error only by about 10–20%. In Fig. 7, wavelengths measured by Gerstmann and Griffith [10] during condensation of Freon-113 on a downward facing flat plate are also plotted. Data compared within about 2% of the prediction based on mean depth of the condensate film. The predicted wavelength would have been about 20% longer if the condensate film had been assumed to be infinite.

* At higher flow rates the liquid started to leave the nodes of Taylor wave in the form of jets. To accommodate large flow rates, the Taylor wavepatterns were observed to shift to critical wavelength which is unaffected by liquid viscosity or by finite depth of the liquid layer.

Melting of a horizontal substrate placed beneath a pool of heavier miscible liquid [13]

In certain applications, the melt may be miscible in the overlying liquid (e.g., MgO floor supporting a pool of molten UO_2). The melt removal of the lighter liquid from the melt layer separating the solid from the overlying liquid pool will again be governed by Taylor instability. The hydrodynamics of the melt removal process will govern the interfacial heat transfer or the penetration of the pool into the supporting substrate. Several studies [13, 14] with simulant fluids have been conducted to determine the heat transfer coefficients associated with penetration of volumetrically heated pools into supporting soluble substrate. The experiments conducted by Brinsfield [14], with a pool of Joule heated salt solution overlying a slab of ice, show that water indeed leaves the solid in the form of regularly spaced self buoyant jets. The melt layer is generally much thinner than the overlying liquid pool and the instability of the melt layer can be described by case 4 formulated earlier. Figure 9 shows the dimensionless most dangerous wavelength as a function of melt layer height for pool to melt density ratios of 1.1 and 4 obtained by solving dispersion relation equation (40). The calculations are made when kinematic viscosities of both liquids are assumed to be the same or when one of the liquids is assumed to be inviscid. It is noted that in the absence of interfacial tension, the most dangerous wavelength goes to zero with melt layer thickness. (The critical wavelength for miscible fluids is always zero.) Similar to immiscible liquids, the functional dependence of wavelength on melt layer height as $H_2 \to 0$, is governed by both the kinematic viscosity conditions and the density ratio of the overlying liquid layer and the melt. However, when viscosity of the melt is considered, the effect of viscosity of the overlying liquid pool on the most dangerous wavelength is small. This, as pointed out earlier, is due to the fact that viscous drag in the melt controls the wavelength as melt layer becomes thin. In the asymptotic limit as $M_2 \to \infty$, the longest wavelengths occur. When viscosities of both melt and overlying liquid layer are considered the effect of increased pool to melt

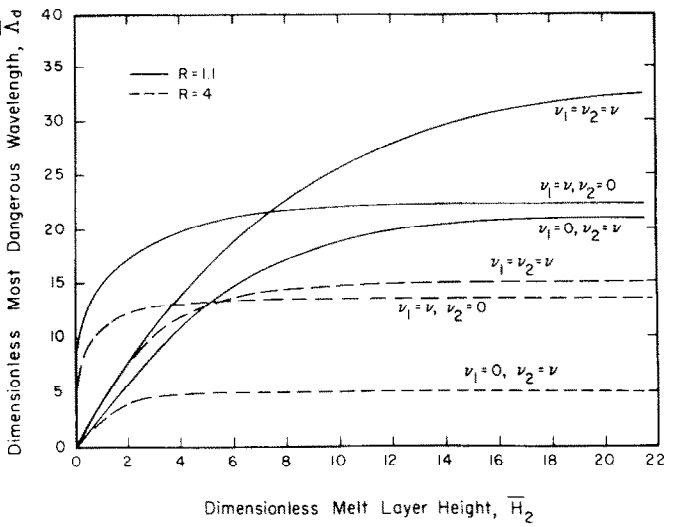

FIG. 9. Effect of melt layer height on the most dangerous Taylor wavelength when melt and the overlying liquid are assumed to be miscible.

density ratio is again to shorten the asymptotic wavelengths.

It may be pointed out that for water at room temperature a 1 mm thick layer would act as infinite whereas for a liquid having kinematic viscosity 30 times greater than water a liquid layer would have to be 1 cm thick to act as infinite. In many practical applications the kinematic viscosity of the melt would be of the same order of magnitude as water and thus a very thin melt layer would act as infinite. For such cases it would be very useful to know the asymptotic value of wavelengths for different melt to pool density ratios. Figure 10 shows such a plot. The non-dimensionalization of the wavelength and the growth rates plotted in Fig. 10 has been modified to include the density ratio. This has been done to bound the wavelengths as pool to melt density ratio goes to unity. However, it has the drawback that for density ratios of the order of 1, the effect of pool to melt density ratio on wavelength is not explicit. It is seen from Fig. 10, that as density ratio $R \rightarrow 1$, the predicted wavelengths are the same when either melt or the overlying liquid pool is assumed to be inviscid. This is indicative of the fact that when pool and melt densities are nearly equal, the interfacial disturbances are affected equally by the hydrodynamic conditions on either side of the interface. For large values of R, the viscosity of the melt layer does not affect the most dangerous wavelength and the corresponding growth rate. Now, as was the case for immiscible liquids, the buoyancy and the

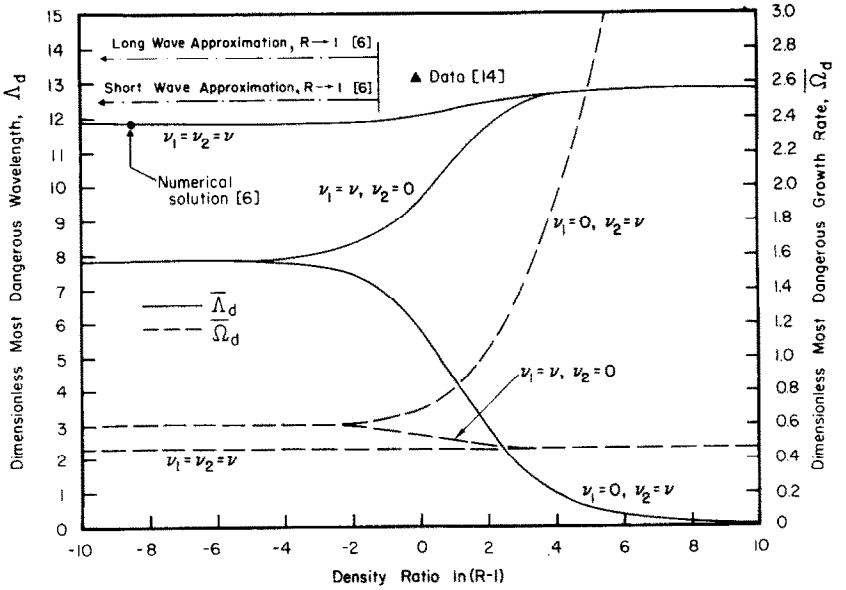

FIG. 10. Dependence of the most dangerous Taylor wavelength for miscible liquids on melt to overlying liquid density ratio.

viscous drag in the pool determine the growth rate and wavelength of the disturbance most susceptible to growth.

In Fig. 10, the most dangerous wavelengths obtained analytically by Plesset and Whipple [6] with long and short wave approximations and for very small density differences are also plotted. It is interesting to note that for density ratios less than 2 [$\ln(R-1) < 0$], their approximate analytical solutions for equal pool to melt viscosities are within 15% of the numerical solutions and show a correct dependence of wavelength on the density ratio. Surprisingly, their analytical solutions do even better for large density ratios, although the dependence of wavelength on density ratio during transition from small to large density ratio is not predicted from their analysis. Plesset and Whipple also solved numerically the dispersion solution, similar to equation (35) for density ratios of 1.00012 and 1.5. Their numerical results agree quite well with the present calculations. The spacing of water jets leaving the surface of the ice slab placed beneath a pool of electrolyte ($R \simeq 1.6$) reported by Brinsfield [14] is also plotted in Fig. 10. It is noted that Brinsfield's data compare favorably with the present predictions in which kinematic viscosities of both liquids are assumed to be the same.

CONCLUSIONS

1. Predictions of the most dangerous Taylor wavelength have been made to include the combined effect of fluid viscosity, fluid layer height and surface tension. It is also shown how the dispersion relations for immiscible fluids can be modified to treat the miscible fluids.
2. In general, the effect of finite vapor layer during film boiling and finite liquid layer during condensation or melting is to shorten the most dangerous wavelength. However, during film boiling very thin vapor layers have been found to behave as infinite.
3. The effect of melt or condensate viscosity is to elongate the most dangerous wavelength, but certain combinations of liquid layer viscosity and height can yield wavelengths which are shorter than predicted from inviscid infinite layer analyses.
4. Dripping experiments with silicone oils have been conducted to determine the combined effect of liquid layer height and viscosity on Taylor wavelength observed during condensation or evaporation. The data have been found to compare well with the predictions.
5. Predicted Taylor wavelengths for miscible liquids have been found to compare favorably with limited data available from experiments conducted to simulate penetration of molten UO_2 into a layer of sacrificial material.

REFERENCES

1. G. I. Taylor, The instability of liquid surfaces when accelerated in a direction perpendicular to their planes—Part I, *Proc. R. Soc.* **A-201,** 192–196 (1950).
2. R. Bellmann and R. H. Pennington, Effects of surface tension and viscosity on Taylor instability, *Q. Appl. Math.* **12,** 151–162 (1954).
3. V. K. Dhir and J. H. Lienhard, Taylor stability of viscous fluids with application to film boiling, *Int. J. Heat Mass Transfer* **16,** 2097–2109 (1973).
4. D. Y. Hsieh, Effects of heat and mass transfer on Rayleigh–Taylor instability, *J. Bas. Engng* 156–162 (1972).
5. H. Lamb, *Hydrodynamics.* 6th edn, pp. 623–625. Dover, New York (1945).
6. M. S. Plesset and C. G. Whipple, Viscous effects in Rayleigh–Taylor instability, *Physics Fluids* **17,** 1–7 (1974).
7. V. Sernas, J. H. Lienhard and V. K. Dhir, The Taylor wave configuration during boiling from a flat plate, *Int. J. Heat Mass Transfer* **16,** 1820–1821 (1973).
8. V. K. Dhir, J. N. Castle and I. Catton, Role of Taylor instability on sublimation of a horizontal slab of dry ice, *J. Heat Transfer* **99,** 411–418 (1977).
9. K. Taghavi-Tafreshi, V. K. Dhir and I. Catton, Thermal and hydrodynamic phenomena associated with melting of a horizontal substrate placed beneath a heavier immiscible liquid, *J. Heat Transfer* **101C,** 318–325 (1979).
10. J. Gerstmann and P. Griffith, Laminar film condensation on the underside of horizontal and inclined surfaces, *Int. J. Heat Mass Transfer* **10,** 567–580 (1967).
11. D. Yung, J. J. Lorenz and E. H. Ganic, Vapor liquid entrainment in shell and tube evaporators, Paper No. 78-WA/HT-35, presented at Winter ASME Meeting held in San Francisco (December 1978).
12. J. H. Lienhard and P. T. Y. Wong, The dominant unstable wavelength and minimum heat flux during film boiling on a horizontal cylinder, *J. Heat Transfer* **86,** 220–226 (1964).
13. H. Werle, Experiments for the diffusion of a volume heated melt in a soluble bed, Karlsruhe Nuclear Research Center, EURFNR-1446 (February 1977).
14. W. A. Brinsfield, Heat transfer from a heated pool to a melting miscible substrate, M.S. Thesis, UCLA (1979).

APPENDIX A
TRANSFORMATION OF DISPERSION RELATIONS FOR IMMISCIBLE LIQUIDS TO MISCIBLE LIQUIDS

The dispersion relations developed for immiscible liquids can easily be adapted for miscible liquids (no interfacial tension) if multiplier, s, of K^3 in function F is set equal to zero. In miscible liquids, the surface tension has no meaning and if one defines new variables such that

$$\bar{\Omega} = \Omega M_i^{-1/3}\left(\frac{R-1}{R+1}\right)^{1/2} \tag{A-1}$$

$$\bar{K} = KM_i^{-2/3} \qquad i = 1 \text{ or } 2 \tag{A-2}$$

$$\bar{H} = HM_i^{2/3} \tag{A-3}$$

Surface tension simply cancels out as far as transformed variables are concerned. The transformed variable becomes

$$\bar{\Omega} = \omega(\nu_i/g^2)^{1/3} \tag{A-1a}$$

$$\bar{K} = k(\nu_i^2/g)^{1/3} \quad i = 1 \text{ or } 2 \tag{A-2a}$$

$$\bar{H} = h(g/\nu_i^2)^{1/3} \tag{A-3a}$$

With these transformations it is seen that surface tension also cancels out in the various parameters except Ω^2 and F appearing in the dispersion relations [e.g. (27)] such as

$$m_j = \left(1 + \frac{\bar{\Omega}}{\bar{K}^2}\frac{\nu_i}{\nu_j}\right) \quad \begin{matrix} i = 1 \text{ or } 2 \\ j = 1 \text{ and } 2 \end{matrix} \tag{A-4}$$

$$\frac{M_1}{M_2} = \frac{\nu_2}{\nu_1} \tag{A-5}$$

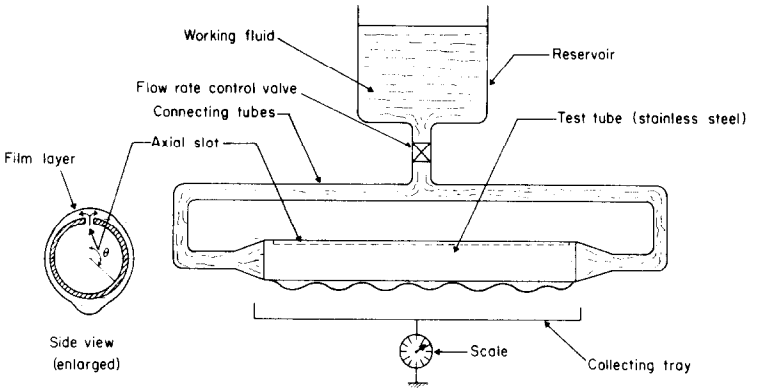

FIG. B.1. Schematic diagram of the apparatus used in dripping experiments.

$$KH_j = \bar{K}\bar{H}_j = kh_j \quad j = 1 \text{ and } 2. \tag{A-6}$$

The terms Ω^2 or $F - \Omega^2$ appear in all the elements of a row of a determinant representing a particular dispersion relation. In terms of the new variables Ω^2 and F are written as

$$\Omega^2 = \bar{\Omega}^2\left(\frac{R+1}{R-1}\right)M_i^{2/3} \quad i = 1 \text{ or } 2 \tag{A-8}$$

$$F = \bar{K}M_i^{2/3}. \tag{A-9}$$

Thus $M_i^{2/3}$, could be factored out from all the elements of that row without any loss of generality. The new dispersion relation in transformed variables will be for miscible liquids. (See for example dispersion relation equation 40.)

APPENDIX B
DRIPPING EXPERIMENTS

A few dripping experiments were conducted to determine the effect liquid viscosity and liquid layer thickness have on the most dangerous wavelength during condensation or evaporation. Different grades of silicone oils were used as test liquids. A 1.25 cm dia stainless steel tube with a longitudinal slot cut at the top was held horizontally. Silicone oil was allowed to enter at a controlled rate into the tube at the two ends of the tube and to flow out of the tube through the slot. Figure B-1 shows a schematic diagram of the apparatus. To obtain longitudinally uniform flow out of the slot, the width of the slot is cut such that pressure drop across the slot is much more than pressure drop in the tube itself. The dripping rate of the liquid was obtained by collecting the liquid in a pan for a certain time and weighing it. Knowing the liquid flow rate per unit length of the slot, Γ, the thickness, δ, of the film around the slab was calculated as

$$\delta(\theta) = \left[\frac{3}{2}\frac{\Gamma\nu}{\rho g \sin\theta}\right]^{1/3} \tag{B-1}$$

where θ is measured from the upper stagnation point of the tube. From equation (B-1), the film thickness, δ, is predicted to become infinitely large all along the tubes as $\theta \to \pi$. However, because of Taylor instability, the liquid film starts to break up at regularly spaced nodes. The film thickness in between these nodes stays finite. Thus, while plotting the wavelength data, the film thickness evaluated as $\theta = 5\pi/6$ was used. This value of film thickness was also found to compare very well with the film thickness observed from the photographs.

INSTABILITE DE TAYLOR DANS L'EBULLITION, LA FUSION, LA CONDENSATION OU L'EVAPORATION

Résumé—On étudie les effets combinés de la tension interfaciale, de la viscosité du liquide et de l'épaisseur de la couche liquide sur l'instabilité de Taylor des interfaces plans et horizontaux. L'analyse linéaire tient en compte l'application potentielle des résultats aux mécanismes physiques tels que l'ébullition, la fusion de substrats horizontaux placés contre des bains de liquides miscibles ou non et la condensation ou l'évaporation à partir de plaques et de tubes horizontaux. Dans tous les cas, les longueurs d'ondes calculées comme les plus dangereuses sont comparées avec les résultats expérimentaux disponibles et avec les résultats analytiques tant que possible. Peu d'expériences ont été faites pour éclaircir l'effet de la viscosité du liquide pendant l'égouttage à partir de tubes horizontaux.

DIE TAYLOR-INSTABILITÄT BEIM SIEDEN- SCHMELZEN UND KONDENSIEREN ODER VERDAMPFEN

Zusammenfassung—Der kombinierte Einfluß von Oberflächenspannung Viskosität der Flüssigkeit und Dicke der Flüssigkeitsschicht auf die Taylor-Instabilität an ebenen horizontalen Grenzflächen wurde untersucht. Bei der Durchführung der linearen Analyse wurde die mögliche Anwendung der Ergebnisse auf physikalische Prozesse stets im Auge behalten: Sieden, Schmelzen von Substrat unter nichtmischbaren und mischbaren Flüssigkeiten, Kondensation oder Verdampfung an horizontalen Platten oder Rohren. In allen Fällen wurden die berechneten gefährlichsten Wellenlängen mit den verfügbaren experimentellen Daten und—wo das möglich war—mit analytischen Grenzwerten verglichen. Einige wenige Versuche wurden durchgeführt, um den Einfluß der Viskosität der Flüssigkeit beim Herabtropfen von horizontalen Rohren festzustellen.

ТЭЙЛОРОВСКАЯ НЕУСТОЙЧИВОСТЬ ПРИ КИПЕНИИ, ПЛАВЛЕНИИ, А ТАКЖЕ КОНДЕНСАЦИИ ИЛИ ИСПАРЕНИИ

Аннотация — Исследуется совместное влияние поверхностного натяжения, вязкости и толщины слоя жидкости на тейлоровскую неустойчивость плоских горизонтальных межфазных поверхностей. Проведен линейный анализ с целью выяснения возможности использования результатов для описания таких физических процессов, как кипение, плавление горизонтальных подложек, над которыми находятся объемы несмешивающихся или смешивающихся жидкостей, а также конденсация (испарение) на горизонтальных пластинах или трубах. Во всех случаях, где это возможно, дано сравнение расчетных значений критических длин волн с имеющимися экспериментальными данными и с ограниченным числом имеющихся аналитических результатов. Выполнено несколько экспериментов с учетом вязкости жидкости при стекании ее с горизонтальных труб в виде капель.